ANYAGOK VILÁGA MATERIALS WORLD
ISSN:1586-0140

X. ÉVFOLYAM 3. szám 2012 December

X. VOLUME Nr. 3 2012 December

Uray L, *Anyagok Világa (Materials Word)* 10 (3) (2012) 42-58

Healing or sintering of splitting or cracks in W wires

LÁSZLÓ URAY

Institute for Technical Physics and Materials Science

Abstract

Tungsten wires – made by powder metallurgy – are investigated after different heat treatments by torsion, which is especially sensitive to the splitting of the wires. The split propensity is especially large in the "as drawn" wires, but it is much less on wires, preannealed at about 1800K. This "improvement "with annealing is surely due to the more stable grain boundary structure, making the splitting less feasible. If the cracks are present already after the wire drawing process, their possible healing or sintering can start with processes like: a/ enhanced low temperature sintering, b/ segregation to grain boundaries, or c/ "roughness induced crack closure". Since an annealing at about 1800K results in much improvement of the splitting properties, so some cracks, created by torsion in these annealed wires are presented here on SEM pictures made on the polished cross-sections of the deformed wire. The material transport, needed to the healing or sintering of the splits, is investigated by measuring the variations in the solute impurity concentration. The diffusion processes are also considered here to reveal the possible processes for the material transports.

Introduction

The fracture mechanism maps for the refractory metals, like W, Mo, Ta, Nb, Re, are described mostly in [1]. At low temperatures, the recrystallized tungsten is completely brittle and fails by cleavage or by equivalent inter-granular mechanisms, but at higher temperatures, so from about $0.3\times T_{mp}$ ($\approx 800^{o}C$), there is a gradual transition from cleavage to ductile fracture [1]. The temperature of this transition is usually called "ductile-to-brittle transition temperature" (DBTT) [2]. Above this temperature fracture surfaces of rods and wires subjected to tensile- or other tests, display a fibrous aspect containing many radial crevices. The deep crevices are the results of an extensive grain boundary delamination, preceding the complete fracture. Further deformation induces necking of individual fibres, to give a typical knife-edge rupture appearance [2], [3], [4]. In heavily deformed materials, however, the effective DBTT is influenced by several factors, like the mode and rate of the deformation, the grain- or fibre- size or the stress state [2]. According to them, thin tungsten wires become well deformable already at the ambient, when deformed e.g. by torsion or by coiling. However, this ductility of thin wires seems illusory, since cracks may appear in the wires, resulting in the splitting of the wire along the grain- or fibre- boundaries [5], [6].

But this splitting does not mean the failure of the wire yet, since these are usually long, helical splits (Figs.1a, 1b) with no observable change in the metallic cross-section, and e.g. at coiling they can extend to several coils of a lamp spiral (Fig.1c). The splitting along the axial

grain boundaries means only, that during deformation, -especially at torsion - the neighboring longitudinal grains can easily slide on each other, starting a so called “Lüders band” on the wire surface [6], [7], as a sign of the instability of the structure. Similarly, at higher strains delamination or fibrous structure (Fig.1d.) may also occur.

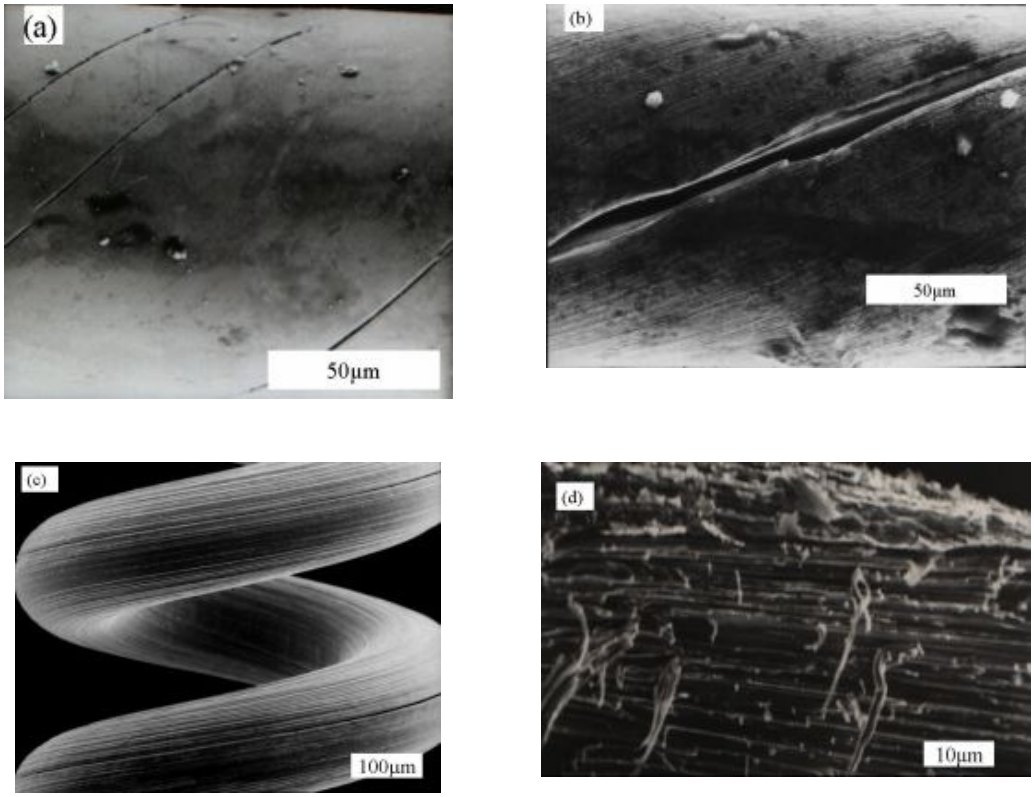

Fig.1. *Deformed wires with splitting - (a) crack- after torsion, (b) deep crack - after torsion, (c) splitting along a lamp spiral, (d) fibrous structure in a wire - after torsion.*

Is the splitting of the W wire an inevitable consequence of the high deformation of tungsten? Undoubtedly, the very high melting point coincides with its low temperature brittleness [1]. In the wire-drawing process of tungsten, (from d_o=14 mm diam. rod to d=0.12 mm diam. wire), the true deformation is as high as $2\times\ln(d_o/d)\approx 9.52$ [8], which increases much the tendency to splitting, stipulated also by the very high energy stored in sub-boundaries, realized in the high dislocation densities [8], [9]. However, this stored energy is partly compensated during wire drawing by inserting several additional annealing stages at appropriate diameters [8]. In materials, subjected to large strain, the mechanisms for the storage of high densities of dislocations and their stability are considered in [10] at strength levels, as high as E/100 to E/50, where E is the Young’s modulus). (For comparison, in heavily drawn tungsten wires (at d≈0.015 mm diam.) the UTS is as high as ≈E/100 [11].)

In these, heavily deformed tungsten wires special properties and structures appear which are not common in the usual soft metals. Among these e.g. the splitting and the fibrous structure of the wires [1], [2], [12] seems mostly responsible for the special properties. Naturally, these properties appear first during wire drawing, but in laboratory circumstances the torsion seems also advantageous, since it is applicable to high deformations, and is especially sensitive to the splitting in the wire. The internal deformation of the wires, and with

it the created atomic size lattice defects are investigated mostly by measuring the electrical resistivity.

Let us mention here the following investigations [13], in which variously doped PM tungsten wires of 0.18 mm diameter, made for lamp filaments, were investigated first of all by torsion. In these experiments, a transformation was found in the properties with the temperature of heat treatments. Especially, it was found, that the "as drawn" wires, or the wires annealed only below about 900°C, shortened during torsion, while the wires, annealed at or above 1100°C, (till 1800°C) elongated during torsion.(the wires are brittle above 2200°C!) This transformation in the elongation properties was confirmed in similar measurements also in [7], where in "as drawn" wires, after some deformation, "plastic instability" was found with the appearance of the so-called "Lüders bands". Since this instability did not appear on annealed wires, it suggested, that the conditions for the instability had to be changed with the annealing, together with changes in the microstructure.

Materials and measurements

Presently, measurements are made on commercial K-Si-Al doped powder metallurgical (PM) tungsten wires of 0.17 mm diameter, made for lamp filament, and the investigations are made partly by torsion, and partly by measuring electrical resistivity. On some wires heat treatments were made at different temperatures by self-resistant heating, usually for 15 min. in a vacuum of 10^{-2} Pa, when the temperature was controlled by the Langmuir tables [15].

2.1 Deformation by torsion

Usually free end torsion tests were made on the wires at the ambient by applying a small load, about 10% of the yield stress.

The torsional loading in the inside of a circular bar with radius, r=a, is described in [14]. The deformation by torsion will be characterized mostly by the surface shear strain, γ:

$$\gamma = \frac{a\,\Theta}{L} \qquad (1)$$

where a is the radius of the wire, θ is the angle of torsion, and L is the gage length of the test specimen. (The maximum surface strain at failure will be called failure strain, $\gamma = \gamma_f$). In a wire with circular cross-section the strain by torsion results in a local stress within the elastic limit [14]:

$$\tau_{z_0} = \frac{G\,r\,\Theta}{L} \qquad (2)$$

where G is the shear modulus, r is the local radius, θ is the angle of torsion and L is the gage length. Equation =(Eq 2.) describes, that the stress is proportional to the local radius, r. However, in plastic materials this proportionality is true only from the core (r=0) up to the elastic-plastic boundary, i.e. to $r = r_{ep}$, and in the plastic region, i.e. at $r_{ep}<r<a$ the stress is almost independent of θ. The first splits usually appear at the surface, where the stress is the highest. The appearance of the splits decreases the surface stress, so at further deformation the stress increases in the depth of the wire, promoting by this the penetration of the splits.

The deformation by torsion is usually characterized by measuring the surface shear strain, γ (Eq 1.). However, the torsional instrument can measure also the surface stress on the wire,

by comparing the apparent stress with that of a standard stainless steel wire series, added to the instrument.

2.2 Electrical resistivity

The deformation of the material- by wire drawing or by torsion generally increases the density of the atomic size lattice defects, which may be e.g. point defects, dislocations, or grain boundaries, but with them the macroscopic defects also appear in the wires, like the porosity or the splitting. After suitable preparations the macroscopic defects could be observed directly e.g. by TEM or by SEM, but the average effects of the of the atomic size lattice defects could be determined more conveniently by measuring also some material properties, like e.g. yield strength [16], or electrical resistivity [17]. Presently the electrical resistivity will be applied for the control of the creation of the lattice defects. But instead of the resistivity, directly only the electical resistance R(T), can be measured witch is measured now at two temperatures, i.e. at T and at T_o ≈300K (i.e at room temperature). However in porous and/or split PM materials, the resistance R(T) measures the lattice defects, only together with the the macroscopic defects, like the porosity, or the helical split-lines. Due to this, it was better to measure the ratios of the resistances, now called, rr from which the geometric or macroscopic effects, like porosity or splitting, are dropped. In this way, this ratio of the resistances is about equal to the resistivity ratio (rr) in the bulk metal:

$$rr = \frac{R(T)}{R(T_0)} \approx \frac{\rho_{bulk}(T)}{\rho_{bulk}(T_0)} \qquad (3)$$

The excess resistivity in the bulk, $\Delta\rho_{bulk}$, is nearly independent of temperature due to the Matthiessen's rule, [18], and it measures the average concentration of solute impurities and/or atomic size lattice defects, created e.g. by wire drawing or by torsion [17].

Supposing, the Matthiessen's rule [18] holds, the excess resistivity of the bulk metal, $\Delta\rho_{bulk}$ could be calculated from the resistivity ratios rr (Eq 3.) which is rr for the specimen, and rr_w, for the pure, zone melted W, as described in [17], like this:

$$\Delta\rho_{bulk} \approx \rho_W(T_0)\frac{rr - rr_w}{1 - rr} \qquad (4)$$

Some properties, measured on the selected wires, A, B and C

For the present measurements the wires were selected after annealing them at 1800K for 15 min. in a vacuum of p ≈10^{-2} Pa, aimed at revealing the splitting properties in the annealed state.

Between the wires the following characteristic differences could be found, measured by their surface shear strain, γ:

A is the best deformable wire, up to γ ≈2, without splitting,
B is somewhat less deformable, it splits already at γ≈ 1-1.5
C is a split wire, on which splitting could be seen already without deformation.

3.1. Transformations in the elongation properties

For this investigation the relative length changes ΔL/L of the wires were measured during torsion, against the surface shear strain γ on "as drawn" wires (Fig.2a) and on annealed wires (Fig.2b)

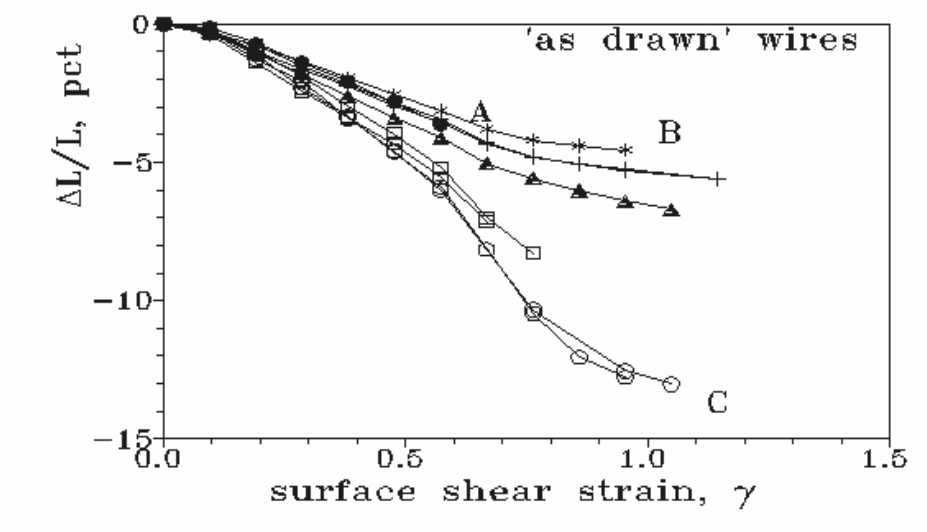

Fig.2a. *ΔL/L vs. γlines on "as drawn" wires, (each shortened during torsion.)*

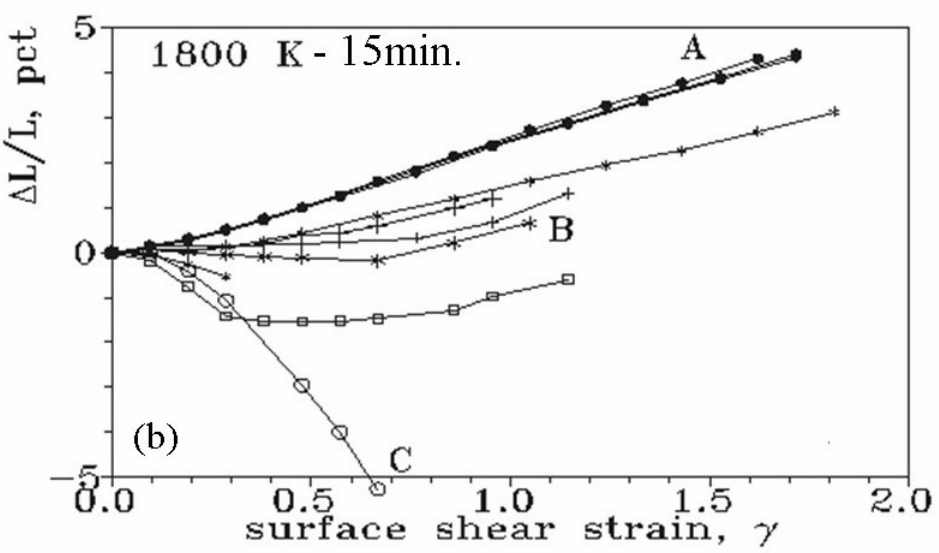

Fig.2b. *The ΔL/L vs. γlines on wires annealed at 1800K for 15 min.*

As one can see, the "as drawn" wires (Fig.2a.) each shortened with torsion. However, the wires, annealed at 1800K for 15 min (Fig.2b) behave differently, depending on their degree of splitting. Namely, the "good quality" annealed wires, like wire A, usually elongate with torsion, while the heavily split wire C, shortens. The partly split wires, like wire B, have the tendency to elongate at higher γ values, depending on their splitting ratio. Summarizing, the measured variations in the elongation properties (Figs.2a and 2b.) prove, that with heat

treatment (now at 1800K) a transformation occurs in the elongation properties (from shortening to elongation) in agreement with [13] and [7], which may serve as a quality control for the splitting properties of the wires.

If the "transformation" is due to the splitting in the fibre structure [1], then it is worth to compare it to a model of the 10×0.1mm stranded copper wires [19], (or "cable"). During torsion "the cable" shortens simply due to the sliding of the constituent wires on each other. This may be similar to the shortening of the "as drawn" tungsten wires in Fig.2a, if these wires are axially split (as in Figs.1a, 1b, or 1c.) At the same time, the single copper wire, with diameter of 0.3 mm, elongates during torsion [19], similarly to the annealed tungsten wire, A, in Fig.2b.

3.2. The stress-strain curves on "as drawn" wires

Measuring also the stresses on the wires (Eq 2.) the stress-strain curves can also be shown (Fig.3.):

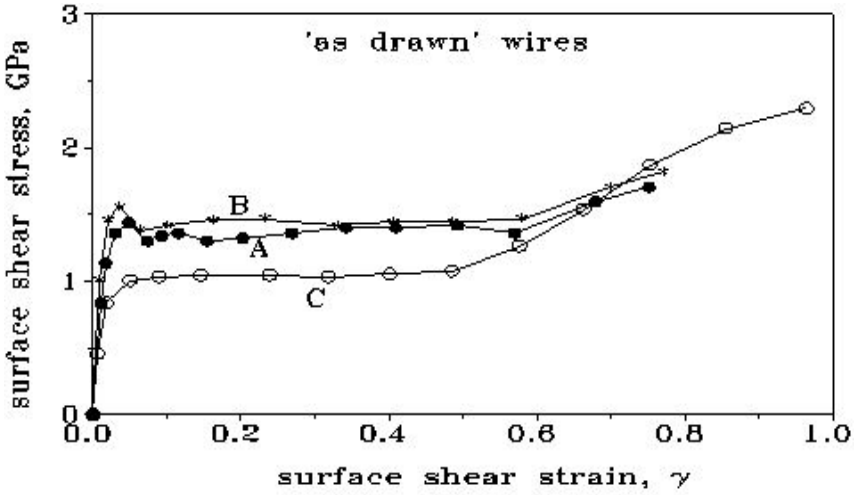

Fig.3. *The stress-strain curves measured by torsion on the "as drawn" wires.*

In case of the wires, A and B, maxima were found at $\gamma \approx 0.04$ surface strains. These are the so-called yield points, at which the first splits appear on the wire surface. No maximum can be seen on the curve of wire C, because this wire was heavily split already at the start. (Like Fig.1b.)

3.3. The internal distribution of the lattice defects in the wires after torsion

The concentration of the atomic size lattice defects can be determined by measuring the excess electrical resistivity, $\Delta\rho_{bulk}$, in the bulk metal, (Eq(3).). For this measurement, the wires, A,B and C were annealed at 1800K for 15 min., and then deformed by torsion uniformly up to $\gamma=0.75$. After this, the diameters of the wires were decreased step by step by electro-polishing, while the resistivities, $\Delta\rho_{bulk}$, were measured on them after each step. The changes in the average radius, Δr, were controlled also by measuring the changes in the weight, Δm, of the specimen. ($\Delta r/r \approx \frac{1}{2}\times\Delta m/m$). The excess resistivities in the removed

layers, $\Delta\rho_{b.layers}$, were calculated in each step, by applying the rule for parallel conductors, like in [17], and the results are presented here in Fig.4.

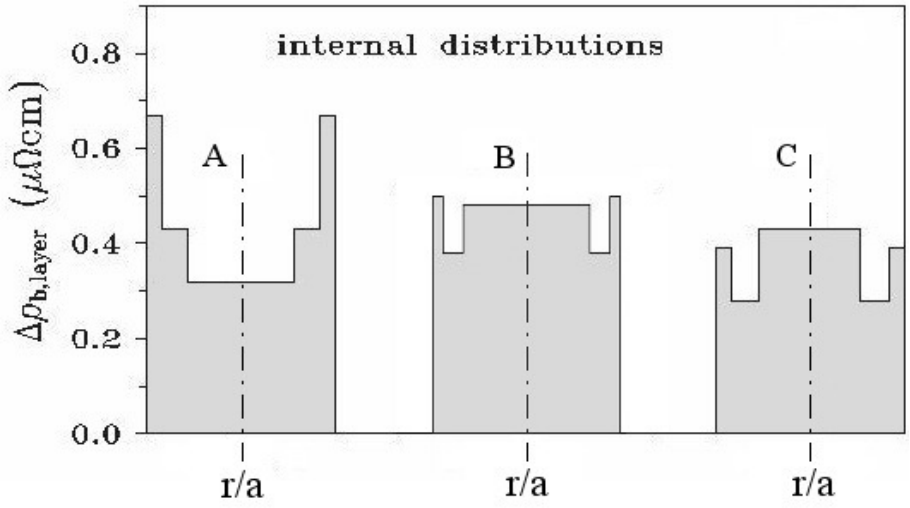

Fig.4. *The internal distribution of atomic size lattice defects in wires A, B and C, annealed at 1800K for 15 min, deformed by torsion to γ=0.75, measured and calculated by electrical resistivity, $\Delta\rho_{bulk}$, in the layers.*

Since at torsion the stress is the largest at the surface of the wire (see Eq. (2), the surface layers are expected to be deformed the most. This is true in case of wire A, but in cases of wires B and C the variations are more flat, revealing even minima, which may indicate splitting during torsion.

3.4. The total concentration of lattice defects, created by torsion

For this measurement the wires A, B and C were annealed at 1800K for 15 min., and then they were deformed by torsion. The measured excess resistivities, $\Delta\rho_{bulk}$, are presented in Fig.5., against the surface strain, γ.

The slopes of the $\Delta\rho_{bulk}$ (γ) straight lines are larger for wires A and B, but less for wire C, suggesting that in the split wire C, the number of the created lattice defects is somewhat less, due to the sliding of the metal along the cracks.

The investigation of crack-profiles in the cross-sections of the wires

In these investigations the wires, A, B and C, were annealed at 1800K for 15 min, and then deformed by torsion up to the failure strain, $\gamma=\gamma_f$, i.e. to γ_f =1.8, 1.4 and 0.8 for the wires A, B and C (like in Fig.5.). After that, the wires were cut far from the failure site. The cut surfaces were then polished to high depth (to about 10 times the diameter), to avoid the rise of new cracks due to the cutting.

Then the cross-sections were finely polished, and investigated by SEM. The pictures are presented here in Figs. 6 a, b, c, and d).

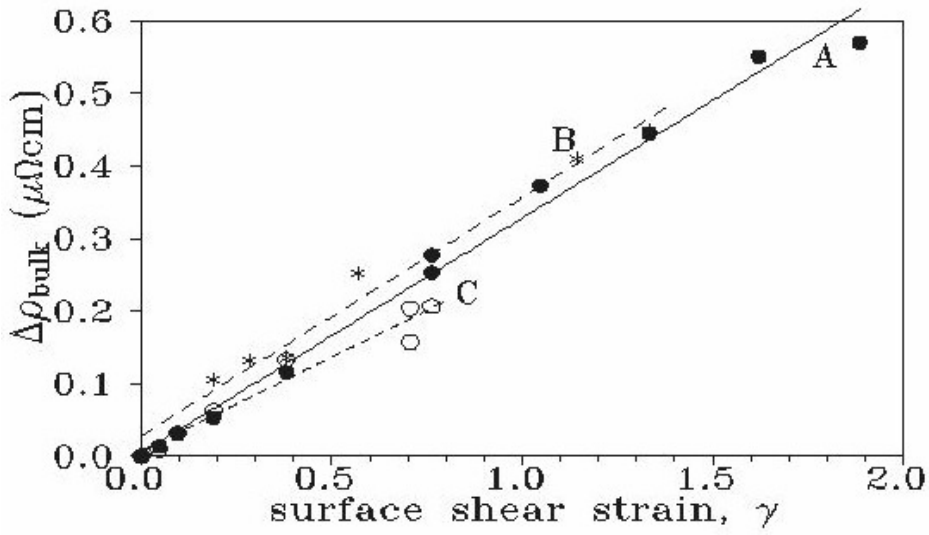

Fig.5. *The excess resistivities, $\Delta\rho_{bulk}$, are shown against the surface shear strains, γ in wires A,B and C, annealed at 1800K for 15 min., and then deformed.*

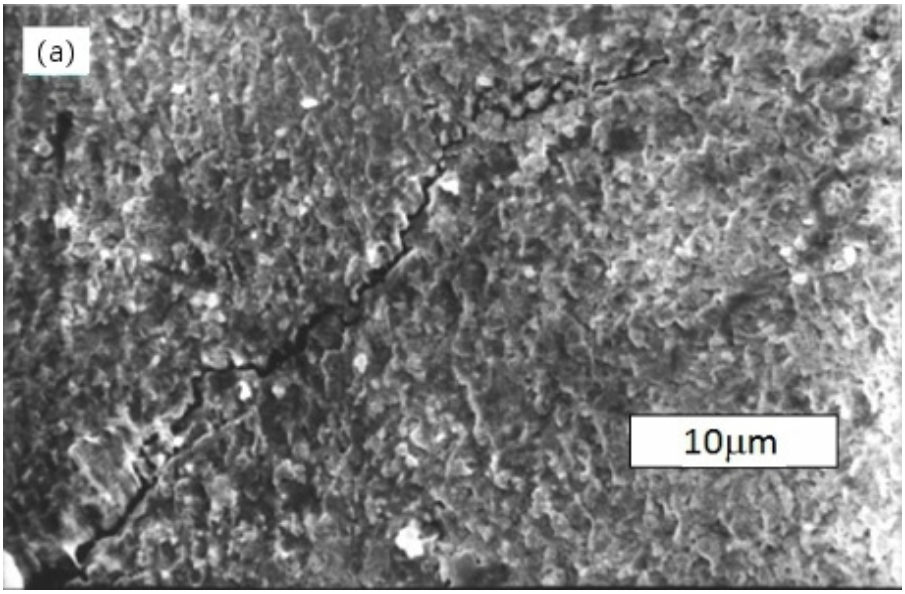

Fig.6a. *Cracks in the cross-section of the annealed and deformed wire A*

Recently the fractal dimension D, [20] or the roughness exponent, H, [21] have widely been used to measure the roughness of fracture surfaces, and correlations were found between the roughness and the fracture energy or toughness of the specimen. In the present crack-profiles, the roughness seems to be the most significant in case of wire A (Fig.6a.), while in wire C (Fig.6.c.) the crack-lines seem almost straight from the surface to the core, like at cleavage.

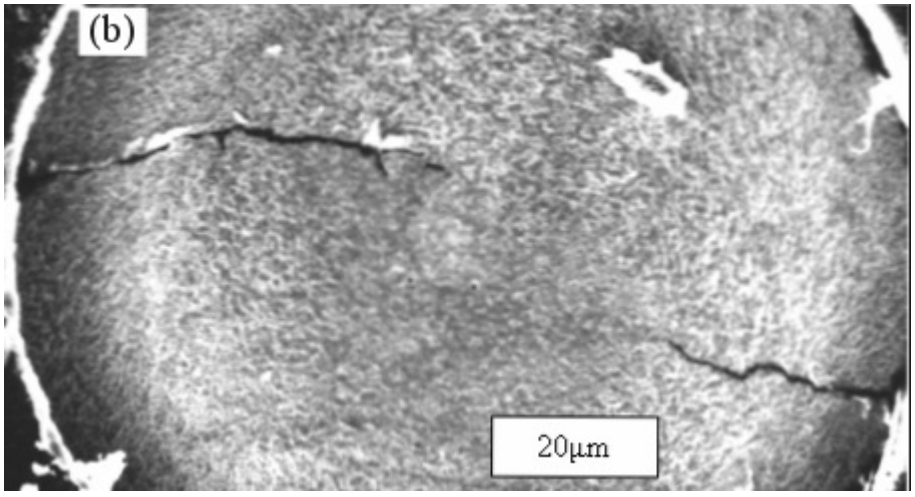

Fig.6b. *Cracks in the cross-section of the annealed and deformed wire B*

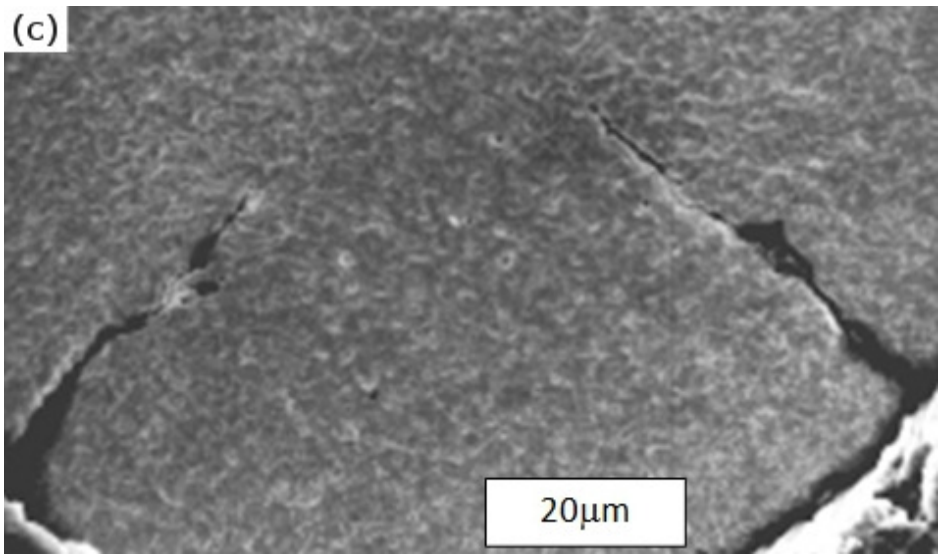

Fig.6c. *Cracks in the cross-section of the annealed and deformed wire C.*

A part of the SEM picture, made on the annealed wire A, (Fig.6a.) is magnified here to illustrate the role of roughness on he sintering of the cracks:

The two sides of the crack resemble to each other along he crack-line, having similar roughness on both sides. Removing the stress of torsion, the two sides can approach each other, so some contacts may appear between them, and at further annealing diffusion is possible at the contact-points, which can make the material stronger. Naturally, this reinforcement may help the healing or sintering of the cracks in the further life of the wire. This is about he same, as the so called “roughness-induced crack closure”, described in [22], which may accelerate the process of sintering at the accidental points of contacts.

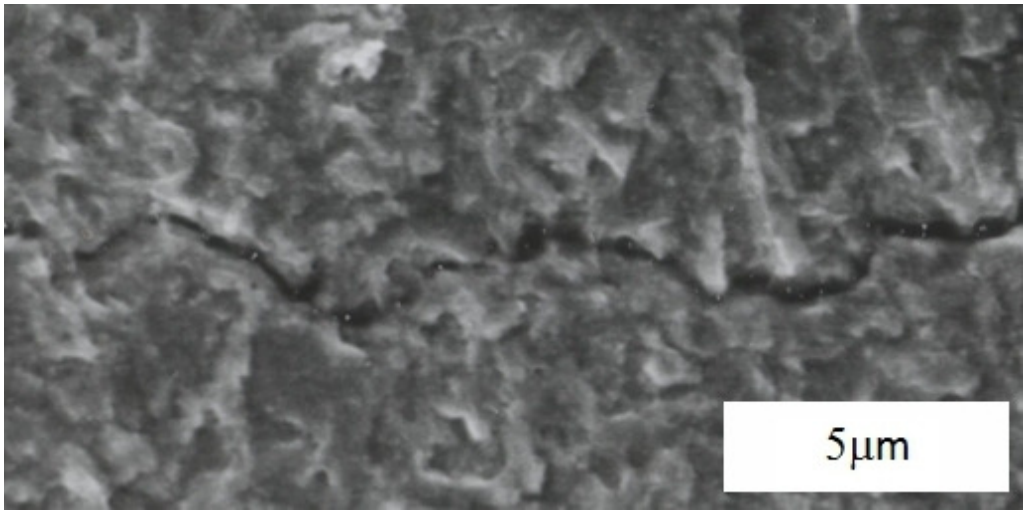

Fig.6d. *Annealed and deformed wire, A. (a part magnified about 2 times, to emphasize the roughness of the crack)*

The annealing diagram, measured on the tungsten wires

If the "transformation in the properties" after annealing at about 1800K is due to the decrease in the lattice defect concentration, or due to a change in the grain boundary structure, it can be seen on their annealing diagrams. Therefore the selected A, B and C wires were annealed at different T(K) temperatures, and the measured $\Delta\rho_{bulk}$ vs. T annealing diagrams are presented here in Fig.7.

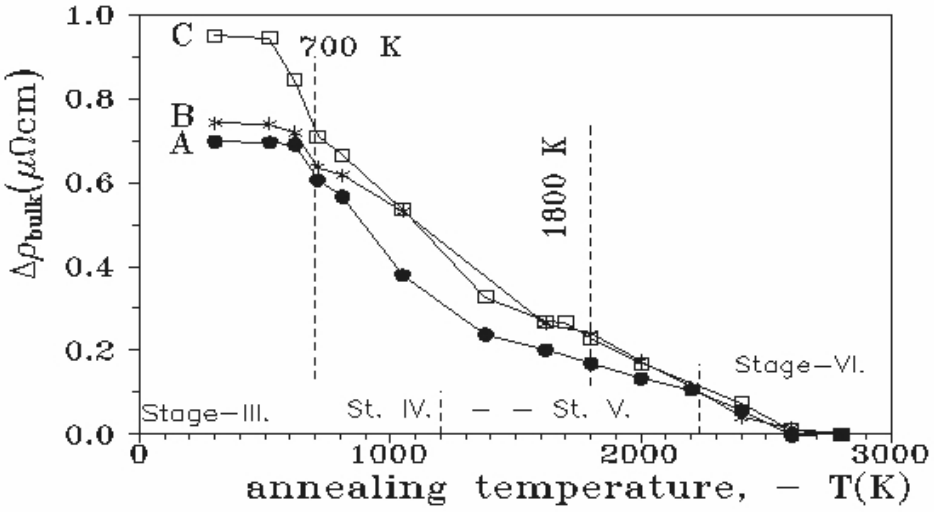

Fig.7. *The annealing diagrams of the excess resistivities, $\Delta\rho_{bulk}$, against the annealing temperatures, T(K), on wires A, B and C.*

In tungsten wires, the excess resistivity decreases in stages, corresponding to the types of the annealed lattice defects. The stages, denoted by III. to VI. on the diagram, correspond approximately to the stages, described in [23], [16], [24]. Stage III. is mainly due to point defects, like in irradiated wires [25], which is ending at T≈700K, as marked. The stage III. recovery is especially large in wire C, suggesting an especially low wire drawing temperature

in this wire, which might be the reason for its large splitting, (like in Fig.1b.). Mechanical strength and yield stress have only less effects on stage III., but their effects are more on stages IV. and V. [16], [24]. Stages V. and VI. are much influenced by the specific impurities of the non-sag wires, and stage VI. is due to the so-called exaggerated grain growth in doped tungsten wire [26]. The annealing diagrams can be seen also after torsion [29], or after coiling [16]. In them stage III. is also prominent, and occurs near to 700K, like in [25].

The relaxation of grain boundaries starts at about 700 K, and the grain boundaries become mostly stress-free after annealing at 1200K for 15 min. [8], [9]. Stage V. is considered mostly as the range of homogeneous grain growth, at which $\Delta\rho_{bulk}$ is proportional to the grain boundary area per unit volume, i.e. to the density of grain boundaries. [27] After annealing at 1800 K for 30 min., the TEM reveals totally relaxed grain boundaries and a homogeneous grain structure with a mean grain diameter of about 1 μm, while the grain interiors are all dislocation-free [9]. This temperature, T≈1800 K, marked also in Fig.7., may be called the temperature of the so-called "primary recrystallization".

Special investigations were made by TEM to see the cross-section of the wires in [27]. In "as drawn" wires the grain-tubes are about lamellar, but at about 1600 K they become rounded, almost hexagonal, mostly with about 60° angles to each other. The rounding of the axial grains at about 1 μm grain size appears also as a "size effect"-maximum in the excess resistivity [28].

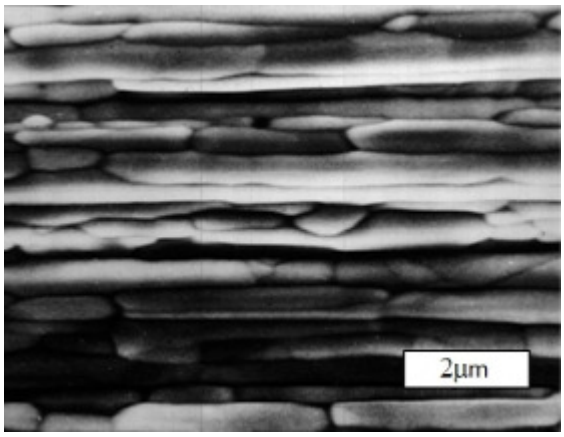

Fig.8. *Stabilized axial grain boundary structure with about 1 μm grain size, after annealing at 1800 K for 15 min*

The appearance of cracks or micro-cracks in the wires

After the usual wire drawing process the material is highly deformed with the development of high internal stresses, realized in high dislocation densities in the "as drawn" state, first of all along fibre boundaries [8], [9].

The tendency to splitting is enhanced by a very high surface energy stored in sub-boundaries in the process of plastic deformation [8]. The effective surface energy for splitting is provided by a strong rise of the dislocation density, which is the highest in the "as drawn" wires, in which cracks may appear directly, already in the process of wire drawing [8]. Pre-existing cracks may spread under the influence of the forces applied to the body, if the work done is at least equal to the increase of the surface energy [12]. In case of precipitation hardening, the rate of work hardening is greater for plate-shaped particles, than for spheres [12].So in [27] in the "as drawn" wires, the observed nearly plate-shaped grains in the cross-

sections have possibly increased stress in one direction. It is also possible, that the wires contain also micro-cracks, or so called ”latent splits” [30], which are not easily recognizable on the grooved surface.

The possible healing or sintering of the splits

The transformation of the wires from shortening to elongation (Figs 2a and 2b.) after annealing at 1800K for 15 min. suggests, that in the vicinity of 1800K the splitting of the wires could be healed or sintered., so that the structure of the wires could be improved in this process.

The bulk diffusion cannot be very effective here, since it is too slow at this temperature [31]. However, the grain boundary diffusion can be more effective, especially since the splits lay just along the grain- or fibre-boundaries.

Actually, we can compare the sintering effects of the different diffusion mechanisms by comparing the material transports achieved by them. In effect a so called “enhanced low temperature sintering” was investigated by [32], who added transitional metals to fine W powder, where about 4 mono-layers of Pd was found as the optimal enhancer (from 1200-1700 K). The Pd is followed in series by Ni, Co, Pt and Fe.

The sinterability can be better by applying nano-powder in high energy ball-milling, as in [33]. In that case the 3-4 μm particle-size could be brought to 8 nm in WC grinding media, and the sintering temperature was only 2100 K for 900 min, and a sintered density of 97% was achieved.

Since we made a series of measurements on a wire of W+300 at ppm Co alloy in the temperature range of about 1000 K to 3000 K [34], it seems worthwhile to look them over to see the material transports, as presented in Fig.9.

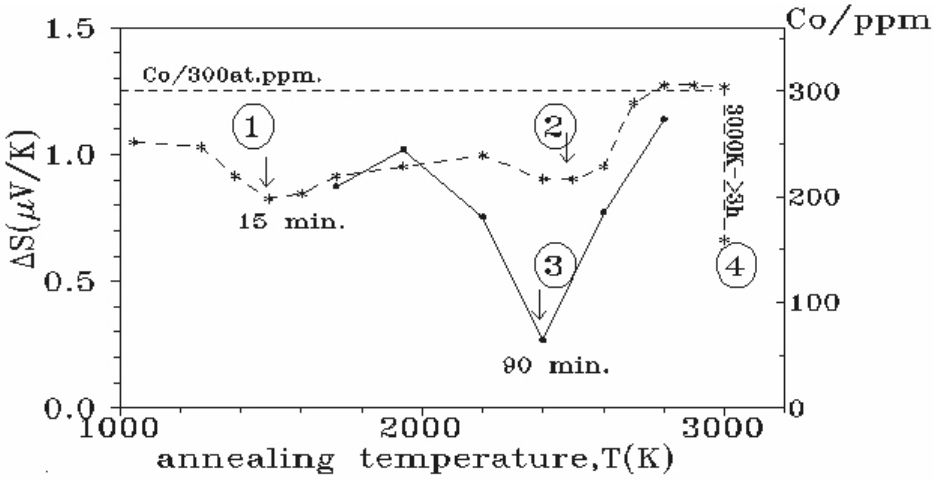

Fig.9. *Material transports in the W-Co wire, measured by thermoelectric power, ΔS. On the curves the dotted and solid lines refer to annealings for 15min. or 90min., respectively.*

The solute Co concentration was measured by thermo-electric power, ΔS(μV/K), which is more sensitive to solute Co, than e.g. to Al, Si, or “lattice defects” [28].

The total Co concentration was controlled by chemical analysis (right scale), and the segregated cobalt, was investigated by AES [34], on the split surfaces.

The main points of the variations in the solute Co concentrations are emphasized by numbers from (1) to (4), like this:

(1)**:** at T≈ 1400 K for 15 min an about 25% deep minimum appeared, in which the solute cobalt segregated partly to the grain boundaries. It was investigated by AES on surfaces, split along grain boundaries, where the cobalt concentration was found 10±5 at. % (0.1 mono-layer) [34]. At this temperature, the segregation is only temporary, since the segregated cobalt goes to solution once again after recrystallization.

(2): at T≈ 2400 K for 15 min) the minimum is permanent, but deepens with increasing annealing time, so:

(3): at T≈ 2400 K for 90 min the solute Co concentration decreased from 300 at.ppm to about 50 at. ppm permanently, as it was proved also by chemical analyses [34]. In this case the solute Co diffuses first to the grain boundaries (1-2 μm grain size, in Fig.8., then by grain boundary diffusion to the surface, from where it can evaporate. This means a significant material transport of Co by grain boundary diffusion.

(4): at T≈3000 K for 3 hours nearly half of the Co evaporated from the wire by bulk diffusion.

The role of diffusion at healing or at sintering

The diffusion in metals is described in [35]. It can be specified for tungsten wires, like this [36]:

Let us have a tungsten wire, with radius a, in which the solute impurity is homogeneously distributed in C_0 concentration.

Annealing this wire at high temperature in vacuum, the solute atoms can diffuse to the surface of the wire, from where they can evaporate. This evaporation is nearly the same for most of the solutes, which evaporate from the surface more easily, than the tungsten atoms do. In tungsten this is true for most of the solutes, like Fe or Co, except e.g. for Re [28].

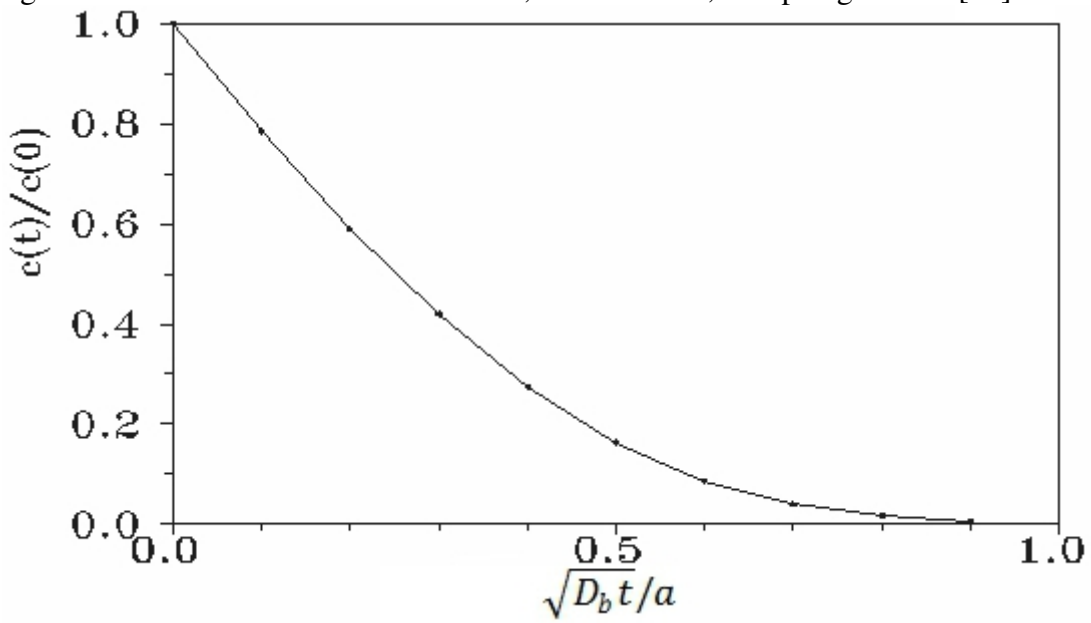

Fig.10. *The evaporation of the solute atoms from a recrystallized tungsten wire. [36]*

After recrystallization, only the bulk diffusion, with diffusion constant, D_b [31] is responsible for the diffusion. However, mainly in the low temperature range, sometimes the

grain boundary or the surface diffusion may be more effective [37], [38]. Their calculation should depend much on the structure and distribution of the grain boundaries and splitting in the wire, so they cannot be calculated here, they will be referred only as more effective ways of diffusion.

In this evaporation process, the usual solutes first take up an "evaporation profile", depending on the parameter, $\sqrt{D_b t}/a$[36]. After this, the relative concentration, c(t)/c(0) of the investigated solute decreases near exponentially with the annealing time, like in Fig.10.

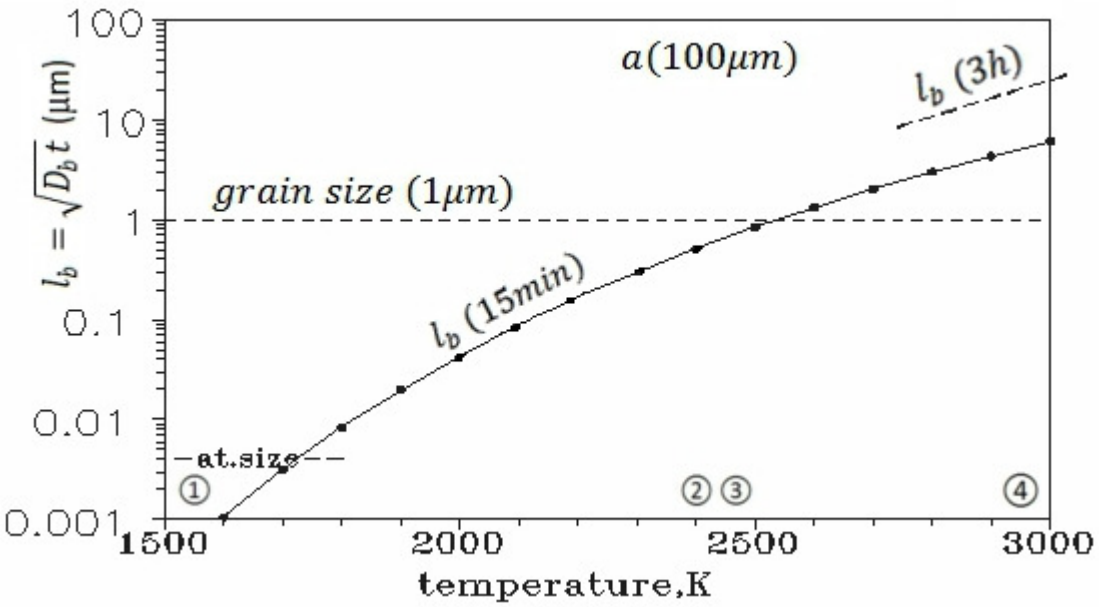

Fig.11. *The "diffusion length"* $l_b = \sqrt{D_b t}$ *(with t=15 min or t=3h) against the annealing temperature T for the WCo wire of Fig.9.*

Most of the solute evaporates from the wire up till, $\sqrt{D_b t}/a \approx 1$ which may be characteristic for the evaporation of the solute (the concentration decreases to about the half at $\sqrt{D_b t}/a \approx 0.25$)

Here $l_b = \sqrt{D_b t}$ is usually called "diffusion length", (having length-dimension), which may be compared to the characteristic lengths in the wire, like its radius, (a≈100μm), the grain size (≈1μm in Fig.8. at 2400K), or the atomic size (3-5nm). This comparison may serve as an illustration for the diffusion processes in the wire, therefore this "diffusion length" $l_b = \sqrt{D_b t}$ (with t=15 min) is presented against the annealing temperature, T, in Fig.11.

The points (1) to (4) in Fig.9. are marked also here at the proper T temperature for better illustration.

According to Fig.9. the enhanced low temperature sintering may set in at about 1400-1500K (1) where the segregation itself [34] needs an effective material transport (moving about 25% of he solute cobalt). However in the bulk diffusion, the diffusion length l_b is only in the range of 0.001-0.01μm so it extends only to a few atomic distances which cannot explain large material transport through the bulk. This may explain the difference between

“healing” and “sintering”. Healing” may mean only a few atomic distances while “sintering” needs some larger material transport.

Therefore at these low temperatures, some other processes must also be considered which are more effective here.

In this way the grain boundary diffusion can be more effective, especially since the splits lay mostly just along the grain- or fibre-boundaries, and above all, the segregation itself was found also on the revealed grain boundaries [34].

Some other possibilities are also enlisted here, which may enhance the low temperature diffusion or sintering, like these:

a/ The extensive movement of grain boundaries and/or dislocations [39], can help the movement of the impurity atoms, and may help also the development of the more stable hexagonal grains, instead of the anisotropic fibres.

b/ The sintering of the cracks can be enhanced also by the process of the so called ”roughness induced crack closure [22]”, suggested also by Fig.6.d. This means, that if e.g. at wire drawing, or at torsion, a crack opened, then after unloading, the same crack may be closed, so at certain points the material may get into contact with the opposite part of the crack, and at these points the diffusion along grain boundaries or fibres makes the connections stronger. Grain boundary or dislocation movements may help this process too. This process may be even more important at micro-splitting, or at ”latent splits” [30], at which only a few atomic opening or fault must be healed.

At T=2400K (2) and (3) are marked, at l_b=1μm, at about the grain size in Fig.8. so l_b=1μm seems enough to move the solute atoms to the grain boundaries, where the grain boundary diffusion is more effective, and it can carry the material to the surface, from where it can easily evaporate even at this temperature T.

At (4) the radius, a, is the critical length, which determines the evaporation of Co at t=3h time (so l_b (3h) is also marked, by dotted line)

Conclusions

This work is connected mainly to the investigation of cracks or splittings present in tungsten wires. The aim of the paper was mainly to reveal the possibility of the healing of the splits or latent splits by sintering. The first step seems to be the mechanical work, which helps to close the cracks, and then to move the dislocations or grain boundaries for their closure. Then the possible annealing processes are shown, which can help to attain significant material transport to help the sintering of the faults. The diffusion is also considered, which can help the healing of atomic size splitting or possibly the “latent splits” too.

Acknowledgements

The author wishes to thank Dr. O. Horacsek for helpful discussions and for making the SEM figures and to V. Varga for the correcture to the figures.

References

[1] Gandhi C. and Ashby M.F.: Acta Met. 27. (1979) pp. 1565-1602.
[2] Morniroli J. P.: in Pink E.: Bartha L. (eds.)
The Metallurgy of Doped/Non-Sag Tungsten, Elsevier Applied Science, New York/London (1989) pp. 235-250.
[3] Schade P.: Proc. 16th Int. Plansee Seminar (Eds.: Kneringer G. Rödhammer P. and Wildner.: Metallwerk Plansee Reutte (2005) V.1.RM16 pp. 168-178.
[4] Lee D.: Met. Trans. A. V.6A. (1975) 2083-2087.
[5] Gaál I., Tóth A. and Bartha L.: Proc. Intern. Conf DF PM (2005) ed.: Parilák L., Danninger H., Stara Lesná IMR SAS Kosice, Slovakia (2005) pp. 175-177.
[6] Gaál I., Tóth A.L., Uray L., Harmat P.: Int. J. Refractory Metals and Hard Materials 24(2006) pp. 325-331.
[7] Szőkefalvi-Nagy Á.: Scripta Met. 16 (1982) pp. 1009-1011.
[8] Milman Yu.V., Zakharova N.P., Ivanschenko R.K., Freze N.I.: Proc. 14th Int. Plansee Seminar Eds.: Kneringer, G., Rödhammer P. and Wilhartitz P., Plansee AG., Reutte (1997) Vol.1. pp.129-147.
[9] Radnóczi G., in Electron Microscopy 1982, Vol.2. Materials Sciences, Proc.10th Int. Congr. on Electron Microscopy Hamburg Aug. 7-24 (1982) p.351.
[10] Embury J. D.: Scripta Met. et Mater. V.27. (1992) pp.981-986.
[11] Smithells C.J.: Tungsten Chapman and Hall LTD (London, 1952)
[12] Kelly A.: Strong Solids Clarendon Press Oxford (1966)
[13] Neugebauer J. in.: Proc. 2nd Internat Symposium on "Reinststoffe in Wissenschaft und Technik": Dresden 1965 Teil.3. (eds.: Kunze J., Pegel B., Schlaubitz K. und Schulze D. Akademie Verlag-Berlin, (1965) pp.755-765.
[14] Bailey J.A.: Fundamental Aspects of Torsional Loading, in: Metals Handbook, V8. Mech. Testing, ASM Metals Park Ohio (1985) pp.139-144.
[15] Langmuir I.: General Electric Review 30, 310, (1927)
[16] Welsch G., Young B.J. and Hehemann R.F.: ICSMA-5th Internat. Conf. on the strength of metals and alloys, Aachen Germany (eds: Hasen P., Gerold V., Kostorz G.): Pergamon Press Oxford, V.3.(1979) pp.1693-1698.
[17] Uray L.: International J. Refractory Metals & Hard Materials 20 (2002) I.pp. 311-318.
[18] Bass J.: In Hallwage K.H., Olsen J.L., (eds) Landolt Börnstein, New Series, III.. 15a Berlin Springer Verlag; (1982) pp.1-288.
[19] Uray L.: Z. Metallkunde, 92 (2001). pp. 386-390.
[20] Mandelbrot B.B. et al. Nature, V.308 (1984) pp.721-722.
[21] Milman V.Y., Stelmashenko N.A. and Blumenfeld R.: Progr. in Mater.Sci.V.38 (1994) pp.425-474.
[22] Wang S.-H. and. Müller C.: Material. Sci. and Eng. A255 (1998) pp.7-15.
[23] Schultz H. Acta Met.12. (1964) pp.649-664.
[24] Szőkefalvi-Nagy Á., Radnóczi G., Nagy A.T., Lipták L., Major J., Gaál I.: in Ortner HM, (ed.) Proc.10th Plansee Seminar Metallwerk Plansee Reutte Austria (1981) V.1. RM31, pp. 193-226.
[25] Seidman D.N.: Scripta Met. 13 (1979) pp. 251-257.
[26] Snow D.B. Metall, Trans A., V. 7a 10a (1976) pp. 783-793.
[27] Barna A., Gaál I., Geszti-Herkner O., Radnóczy G., Uray L. High Temp. - High Press. 10 (1978) pp.197-205.
[28] Uray L.: International J. Refractory Metals & Hard Materials 20 (2002). II.pp.319-326.
[29] Uray L.: High Temp. Mater. and Processes V.16.No.2. (1997) pp. 139-148.

[30] Schob O.: in: Pink E., Bartha L. (eds.) the Metallurgy of Doped/Non-Sag Tungsten Elsevier Applied Science New York/London (1989) 83-112.
[31] Klotsman S.M., Osetrov S.V. and Timofeev A.N.: Phys. Rev. B V.46,(5) (1992-I) pp.2831-2837.
[32] German R.M. and Munir Z.A.: Met. and Mat.Trans.A (Springer Boston) V.7.(11) (1976) pp.1873-1877.
[33] Malewar R., Kumar K. S., Murty B. S. Sarma B., Pabi S.K.: J. Mater. Res. V.22. No.5. (2007) pp.1200-1206.
[34] Uray L., Sulyok A. and Tekula-Buxbaum P.: High Temp. Mater. and Proc.V. 24. No.5. (2005) pp.289-300.
[35] Crank J.: The Mathematics of Diffusion, Clarendon Press, Oxford (1956)
[36] Uray L., Neugebauer J.M., Gaál I.:Acta Techn. Acad. Sci. Hung. V.78 (3-4) (1974) pp.393-404.
[37] Arkhipova N.K., Kaygorodov V.N., Klotsman S.M. and Kozhevina E.V.: J. Appl. Phys. 72 (2) (1992) pp.454-460.
[38] Kozma L. and Bartha L.: Isotopenpraxis 9. Jahrgang 6. Heft (1973) pp.203-205.
[39] Kasen M.B.: Acta Met.V.31 (1983) pp.489-497.